A model of chaperone competition in bacterial gene regulatory networks

Nicholas Nolan[1], Michael Laub[2], and Domitilla Del Vecchio[3]

***Abstract*—Chaperones are a global resource within cellular biomolecular systems, ensuring that proteins are properly folded and preventing that aggregation leads to cell death. Introducing genetic circuits to a cell may place a load on these folding resources, resulting in unintended coupling between otherwise independent circuits' behavior. Previous analyses have considered loading effects on other cellular resources — such as gene expression resources — but have not included chaperone-enabled folding. In this paper, we model two chaperone modalities, encapsulating two important classes of chaperones as well as their potential interactions. We identify distinct responses that arise from the different architectures which can be either competitive or activating. This work indicates that native cellular chaperones may have built-in control architectures to mitigate loading by an increased demand from chaperone-reliant proteins.**

I. Introduction

Across all domains of life, a cell's proteins must be folded properly to function [1], [2]. If a protein misfolds, it may potentially aggregate, leading to cell death [3]. In bacteria, this folding can be accomplished with the help of proteins known as chaperones, which are responsible for the disaggregation and folding of other proteins [1]–[3]. Approximately 20% of protein species in the cell rely on these chaperones to fold; among this 20% are proteins that are critically necessary for a cell's survival, such as amino acid biosynthesis proteins, regulators for important transcriptional pathways, and even other chaperones [4], [5].

Two important general-purpose classes of chaperones are the DnaK/DnaJ/GrpE (KJE) chaperone system, and the GroEL/GroES (ELS) chaperonin system. Both of these systems detect the folding state of a target protein by binding its hydrophobic residues [5], [6]. Correctly-folded proteins tend to consolidate their hydrophobic residues to their interiors, to minimize hydrophobic-hydrophilic interactions with the cytoplasm; therefore unfolded and misfolded proteins (each of which are likely to have exposed hydrophobic residues) are preferentially bound by chaperone systems. The KJE folding system operates by binding to unfolded or misfolded proteins and preventing their aggregation, and — upon unbinding — leaves the protein in an unfolded state, so that it may either fold properly or misfold again [6]. The ELS system, however, plays a more active role in the folding process, by surrounding unfolded proteins in an isolated chamber, allowing the protein to fold in the absence of any external factors [5]. Less-stable proteins rely more on ELS to fold, while proteins that are more stable (but still reliant on chaperones to fold) are able to refold using either KJE or ELS [5].

Recent work has established that competition for resources is a significant factor affecting engineered genetic circuitry, for both bacterial and mammalian cells [7]–[9]. In bacterial systems, it was determined that ribosomes — which are responsible for translating a gene's messenger RNA into unfolded protein — are in high demand, and that competition for ribosomal resources can lead to coupling between seemingly-orthogonal systems [7], [9]. Recent work has suggested that limited folding resources may play a role in preventing cell death in the presence of proteins that are toxic when folded, such as the endoribonuclease toxin MazF [10].

This paper will compare two different models of competition for chaperones, and analyze how biochemical parameters affect the extent of coupling among proteins that rely on the same chaperones. Specifically, we consider two modalities. In modality 1, we abstract chaperone function into a single enzymatic reaction converting unfolded proteins to folded proteins (Fig 1(a)). In modality 2, we divide the chaperone pool into two separate sub-pools and consider that one subprotein of the KJE system is itself reliant on ELS to fold, accounting for differences between KJE and ELS refolding systems (Fig 1(b)) [5]. In each modality, we analyze the ordinary differential equation (ODE) models that correspond to the chaperone folding system, and identify any unintended coupling that results from sharing folding resources. We find that the architecture of modality 1 leads to a competitive effect, in which the increasing the volume of the competitor module leads to a decrease in folding in the module of interest; by contrast, modality 2 can give rise to either the same competitive effect, or an activating effect, in which introducing the competitor module boosts the folding of the module of interest. This ultimately suggests the existence of a circuit architecture that compensates for competition within the cell.

The outline of this paper is as follows: Section II introduces the chemical reactions, modeling framework, and analytical findings of unintended regulatory interactions present

This work was supported by AFOSR grant FA9550-22-1-0316.

[1]Department of Biological Engineering, Massachusetts Institute of Technology, 77 Massachusetts Avenue, Cambridge, MA 02139. Email: ncn@mit.edu

[2]Department of Biology, Massachusetts Institute of Technology, 77 Massachusetts Avenue, Cambridge, MA 02139. Email: laub@mit.edu

[3]Department of Mechanical Engineering, Massachusetts Institute of Technology, 77 Massachusetts Avenue, Cambridge, MA 02139. Email: ddv@mit.edu

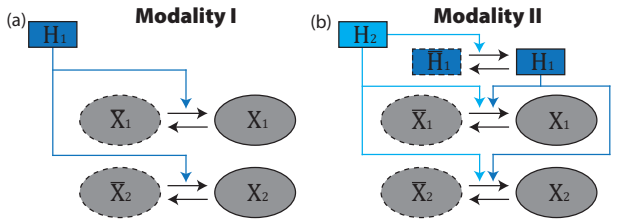

Fig. 1. Models to describe chaperone folding. (a) In modality 1, chaperones are modeled as a single species H_1 and enzymatically convert unfolded proteins ($\bar{X}_i$) into folded proteins (X_i). (b) In modality 2, chaperones are considered in two separate pools of KJE (H_1) and ELS (H_2) systems. The chaperone protein DnaJ of KJE is critically reliant on ELS to fold properly, resulting in a cascaded architecture.

in the model of modality 1. Section III performs a similar analysis of unintended interactions in modality 2. Section IV concludes the study and considers the biologically-relevant findings of the system, lending insight into potential future work that can be done in the field.

II. Modality 1: Single Chaperone Species

In modality 1, the reaction network comprises a single chaperone species H_1, and proteins that need to be folded ($\bar{X}_i$, where $i \in \{1, 2, ..., n\}$). The chaperone species reversibly binds with each $\bar{X}_i$ to form a complex C_i, which can then produce an output folded protein X_i and returns the chaperone to the available pool. It is assumed that there is a fixed, constant pool of each protein X_i in the system, so that production and dilution of proteins is not considered. The following chemical reactions correspond to this model:

$$H_1 + \bar{X}_i \underset{d_i}{\overset{a_i}{\rightleftharpoons}} C_i \xrightarrow{k_i} H_1 + X_i$$
$$X_i \xrightarrow{\gamma_i} \bar{X}_i,$$

from which the following reaction rate equations can be derived using mass action kinetics [11]:

$$\frac{d}{dt}\bar{X}_i = \gamma_i X_i - a_i \bar{X}_i H_1 + d_i C_i \quad (1)$$
$$\frac{d}{dt}C_i = a_i \bar{X}_i H_1 - (d_i + k_i) C_i$$
$$\frac{d}{dt}X_i = k_i C_i - \gamma_i X_i. \quad (2)$$

We have conserved quantities of proteins and chaperones:

$$X_{it} = X_i + \bar{X}_i + C_i \quad (3)$$
$$H_{1t} = H_1 + \sum_{i=1}^{n} C_i, \quad (4)$$

where X_{it} and H_{1t} are the total concentrations of the i-th protein and the chaperone, respectively. The complex formation reaction is fast, and so we may approximate C_i according to its quasi-steady state [11]:

$$C_i = \frac{H_1 \bar{X}_i}{K_i}, \quad (5)$$

where $K_i = (d_i + k_i)/a_i$. Plugging (5) into (4), we find the concentration of free chaperones H_1:

$$H_1 = \frac{H_{1t}}{1 + \sum_{i=1}^{n} \frac{\bar{X}_i}{K_i}}. \quad (6)$$

We substitute (3), (5), and (6) into (1), to arrive at a final set of ODEs for our reduced system describing the dynamics of chaperone-mediated folding of proteins:

$$\frac{d}{dt}\bar{X}_i = \underbrace{\gamma_i(X_{it} - \bar{X}_i) - (\gamma_i + k_i) H_{1t} \frac{\bar{X}_i/K_i}{1 + \sum_{j=1}^{n} \frac{\bar{X}_j}{K_j}}}_{=f_i(\bar{X})}, \quad (7)$$

where $\bar{X} = (\bar{X}_1, ..., \bar{X}_n)$ is a vector of unfolded protein concentrations, and $X_t = (X_{1t}, ..., X_{nt})$ is a vector of total protein concentrations, so that $\frac{d}{dt}\bar{X} = f(\bar{X}) = (f_1(\bar{X}), ..., f_n(\bar{X}))$. By taking the conservation law (3) and substituting our quasi-steady state concentration from (5), we arrive at the concentration of folded proteins:

$$X_i = X_{it} - \bar{X}_i \left(1 + \frac{H_{1t}/K_i}{1 + \sum_{j=1}^{n} \frac{\bar{X}_j}{K_j}}\right). \quad (8)$$

For a state variable X, we will denote its equilibrium value by X^*. We will next show that increasing the total level of a competitor protein X_{jt} causes a decrease in the equilibrium level of folded protein of interest $X_i^*, i \neq j$, and that increasing the total concentration of the protein of interest increases the concentration of the folded protein of interest.

Claim 1. *In the system given by (7), for $n = 2$, we have that:*

$$\left.\frac{\partial X_i}{\partial X_{jt}}\right|_{X_i = X_i^*} \begin{cases} > 0, & i = j \\ < 0, & \text{otherwise.} \end{cases}$$

Proof. We consider the system at equilibrium:

$$0 = \gamma_i(X_{it} - \bar{X}_i) - (\gamma_i + k_i) H_{1t} \frac{\bar{X}_i/K_i}{1 + \sum_{j=1}^{n} \frac{\bar{X}_j}{K_j}}.$$

Without loss of generality, we will take $i = 1$. Taking the Jacobian of the system and evaluating it at the equilibrium, we arrive at the following expression:

$$\left.\frac{\partial f}{\partial \bar{X}}\right|_{\bar{X} = \bar{X}^*} = \begin{bmatrix} g_1 & h_{12} \\ h_{21} & g_2 \end{bmatrix},$$

where:

$$g_i = -\gamma_i - (\gamma_i + k_i) \frac{H_{1t}}{K_i} \frac{1 + \sum_{j \neq i} \frac{\bar{X}_j^*}{K_j}}{\left(1 + \sum_{j=1}^{2} \frac{\bar{X}_j^*}{K_j}\right)^2} < 0$$
$$h_{ij} = (\gamma_i + k_i) \frac{H_{1t}}{K_j} \frac{\bar{X}_i^*/K_i}{\left(1 + \sum_{j=1}^{2} \frac{\bar{X}_j^*}{K_j}\right)^2} > 0.$$

Analysis shows that $\det\left(\frac{\partial f}{\partial \bar{X}}\right) = g_1 g_2 - h_{12} h_{21} > 0$, so this Jacobian matrix is invertible. With this, we apply the implicit function theorem from [12] to consider the effect of X_{2t} on

the equilibrium level of each unfolded protein $\bar{X}_j^*$, and arrive at the following expression:

$$\left.\frac{\partial \bar{X}}{\partial X_{2t}}\right|_{\bar{X}=\bar{X}^*} = -\left(\frac{\partial f}{\partial \bar{X}^*}\right)^{-1}\frac{\partial f}{\partial X_{2t}} \tag{9}$$

$$= \underbrace{\frac{1}{g_1 g_2 - h_{12}h_{21}}}_{>0}\begin{bmatrix}\gamma_2 h_{12}\\ -\gamma_2 g_1\end{bmatrix}. \tag{10}$$

We have from above that $\frac{\partial \bar{X}_1}{\partial X_{2t}} > 0$. Taking the partial derivative of (8) with respect to X_{2t}, we have:

$$\left.\frac{\partial X_1}{\partial X_{2t}}\right|_{\bar{X}_1=\bar{X}^*} = -\left.\frac{\partial \bar{X}}{\partial X_{2t}}\right|_{\bar{X}=\bar{X}^*}\left(1+\frac{\frac{H_{1t}}{K_1}\left(1+\frac{\bar{X}_2^*}{K_2}\right)}{\left(1+\sum_{j=1}^{2}\frac{\bar{X}_j^*}{K_j}\right)^2}\right),$$

and so $\frac{\partial X_1}{\partial X_{2t}} < 0$, which accounts for the lower part of the proof. Considering the upper section, we take the partial derivative of (8) with respect to X_{1t}:

$$\left.\frac{\partial X_1}{\partial X_{1t}}\right|_{\bar{X}_1=\bar{X}^*} = 1 - \underbrace{\left.\frac{\partial \bar{X}}{\partial X_{1t}}\right|_{\bar{X}=\bar{X}^*}\left(1+\frac{\frac{H_{1t}}{K_1}\left(1+\frac{\bar{X}_2^*}{K_2}\right)}{\left(1+\sum_{j=1}^{2}\frac{\bar{X}_j^*}{K_j}\right)^2}\right)}_{=c}.$$

It can be shown that $c < 1$, and so we have $\frac{\partial X_1}{\partial X_{2t}} > 0$, which completes the proof. □

These competition effects are shown in Figure 2(a). As the total concentration of the competitor protein X_{2t} increases, the level of free chaperones H decreases, which in turn leads to fewer available chaperones to assist in the folding of the protein of interest X_1. As H_{1t} increases, competition becomes negligible, as more chaperones are available to assist in folding. Therefore, increasing chaperone concentration can help to mitigate the effects of competition (Figure 2(b)). Now, we continue to an analysis of modality 2.

III. Modality 2: Dual Chaperones in Cascade

Modality 1 implicitly assumes that all chaperone species operate as a single cohesive unit, and that this unit operates comparably on all proteins. It has been shown that this is not the case; not all proteins are equally stable, and not all proteins are folded equally well by all chaperones [5], [14]. This necessitates the development of modality 2, in which we divide this system into 2 different chaperones, encapsulating roughly non-ELS (H_1) and ELS (H_2) chaperone systems. This is because ELS has been observed to operate on more unstable proteins, and non-ELS chaperone systems have been observed to be interchangeable in some contexts [15], [16]. It has additionally been suggested that the DnaJ subunit of KJE is itself reliant on ELS to fold; to incorporate this, we consider that the chaperone species H_1 can unfold into a nonfunctional chaperone $\bar{H}_1$, and be enzymatically refolded by H_2.

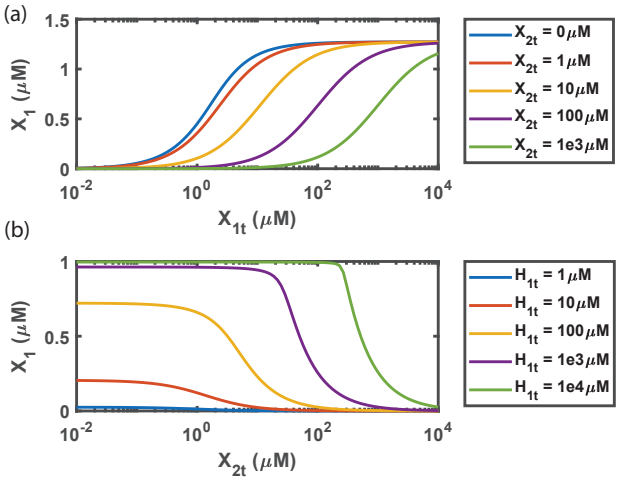

Fig. 2. Modality 1 exhibits chaperone competition, which can be mitigated by increasing the total chaperone concentration in the system. (a) Plots of the equilibrium concentration X_1 as a function of X_{1t} in the presence of a competitor X_2. The input-output relationship between the total concentration X_{1t} and the folded concentration X_1 is a function of X_{2t}. (b) As the total chaperone level increases, the range of concentrations X_{2t} for which the folded level of the protein of interest is independent of X_{2t} expands. Parameters used: $k_i = 4.8\cdot 10^{-1}\text{min}^{-1}$, $K_i = 1\mu$M, $\gamma_i = 0.0119\text{min}^{-1}$, $H_{1t} = 49\mu$M (for (a)), $X_{1t} = 1\mu$M (for (b)).

As a direct result of these changes to the system architecture, we observe that the system has a potential for activating effects, in that the introduction of a competitor protein boosts the folding of the protein of interest. The system can be summarized in the following chemical reactions:

$$\bar{\text{H}}_1 + \text{H}_2 \underset{d_0}{\overset{a_0}{\rightleftharpoons}} \text{C}_0 \xrightarrow{k_0} \text{H}_1 + \text{H}_2$$
$$\text{H}_1 \xrightarrow{\gamma_0} \bar{\text{H}}_1$$
$$\text{H}_j + \bar{\text{X}}_i \underset{d_{ij}}{\overset{a_{ij}}{\rightleftharpoons}} \text{C}_{ij} \xrightarrow{k_{ij}} \text{H}_j + \text{X}_i$$
$$\text{X}_i \xrightarrow{\gamma_i} \bar{\text{X}}_i,$$

from which reaction rate equations can be derived with mass-action kinetics:

$$\frac{d}{dt}\bar{H}_1 = \gamma_0 H_1 + d_0 C_0 - a_0 \bar{H}_1 H_2 \tag{11}$$
$$\frac{d}{dt}C_0 = a_0 \bar{H}_1 H_2 - (d_0 + k_0)C_0$$
$$\frac{d}{dt}H_1 = k_0 C_0 - \gamma_0 H_1 - \sum_{i=1}^{n}(a_{i1}\bar{X}_i H_1 - (d_{i1} + k_{i1})C_{i1})$$
$$\frac{d}{dt}H_2 = \sum_{i=1}^{n}((d_{i2} + k_{i2})C_{i2} - a_{i2}\bar{X}_i H_2)$$
$$\frac{d}{dt}\bar{X}_i = \gamma_i X_i + \sum_{j=1}^{2}(d_{ij}C_{ij} - a_{ij}\bar{X}_i H_j) \tag{12}$$
$$\frac{d}{dt}C_{ij} = a_{ij}\bar{X}_i H_j - (d_{ij} + k_{ij})C_{ij}$$
$$\frac{d}{dt}X_i = \sum_{j=1}^{2} k_{ij}C_{ij} - \gamma_i X_i.$$

We have the following conserved quantities:

$$X_{it} = X_i + \bar{X}_i + C_{i1} + C_{i2} \tag{13}$$

$$H_{1t} = H_1 + \bar{H}_1 + C_0 + \sum_{i=1}^{n} C_{i1} \tag{14}$$

$$H_{2t} = H_2 + C_0 + \sum_{i=1}^{n} C_{i2}. \tag{15}$$

As before, we approximate the enzymatic reaction to be fast, arriving at a similar result as (5) for our quasi-steady state complex concentrations C_0 and C_{ij} [11]. We find the following for the quasi-steady state complex concentrations C_0 and C_{ij}:

$$C_0 = \frac{\bar{H}_1 H_2}{K_0} \tag{16}$$

$$C_{ij} = \frac{\bar{X}_i H_j}{K_{ij}}, \tag{17}$$

where $K_0 = (d_0 + k_0)/a_0$ and $K_{ij} = (d_{ij} + k_{ij})/a_{ij}$. Plugging (16) and (17) into (14) and (15), we arrive at the following expressions for the concentration of free chaperones:

$$H_2 = \frac{H_{2t}}{1 + \frac{\bar{H}_1}{K_0} + \sum_{i=1}^{n} \frac{\bar{X}_i}{K_{i2}}} \tag{18}$$

$$H_1 = \frac{H_{1t}}{1 + \frac{\gamma_0}{k_0}\left(1 + \frac{K_0}{H_2}\right) + \sum_{i=1}^{n} \frac{\bar{X}_i}{K_{i1}}}. \tag{19}$$

From here, we substitute (13), (16), (17), (18), and (19) into (11) and (12) to obtain a reduced ODE model of our cascaded system:

$$\begin{aligned}
\frac{d}{dt}\bar{H}_1 &= \gamma_0 H_{1t} \frac{1}{1 + \frac{\gamma_0}{k_0}\left(1 + \frac{K_0}{H_2}\right) + \sum_{i=1}^{n} \frac{\bar{X}_i}{K_{i1}}} \\
&\quad - k_0 H_{2t} \frac{\bar{H}_1/K_0}{1 + \frac{\bar{H}_1}{K_0} + \sum_{i=1}^{n} \frac{\bar{X}_i}{K_{i2}}} \\
\frac{d}{dt}\bar{X}_i &= \gamma_i (X_{it} - \bar{X}_i) \\
&\quad - (\gamma_i + k_{i1}) H_{1t} \frac{\frac{\bar{X}_i}{K_{i1}}}{1 + \frac{\gamma_0}{k_0}\left(1 + \frac{K_0}{H_2}\right) + \sum_{i=1}^{n} \frac{\bar{X}_i}{K_{i1}}} \\
&\quad - (\gamma_i + k_{i2}) H_{2t} \frac{\frac{\bar{X}_i}{K_{i2}}}{1 + \frac{\bar{H}_1}{K_0} + \sum_{i=1}^{n} \frac{\bar{X}_i}{K_{i2}}}.
\end{aligned} \tag{20}$$

For the sake of analysis, we will take $n = 2$, so that we have two proteins competing to fold with H_1, and all three of $\bar{\mathrm{X}}_1$, $\bar{\mathrm{X}}_2$, and $\bar{\mathrm{H}}_1$ competing to fold with H_2. In this case, we define the non-dimensionalization parameters in Table I,

Term	Definition
$x_{i,f}$	X_i/K_{i2}
x_i	$\bar{X}_i/K_{i2}$
x_{it}	X_{it}/K_{i2}
τ	$\gamma_0 t$
h_1	H_1/K_0
h_{jt}	H_{jT}/K_0
δ_0	k_0/γ_0
δ_i	γ_i/γ_0
α_{ij}	$(\gamma_i + k_{ij})K_0/\gamma_0 K_{ij}$
Ω_0	$1 + h_{2t} + \delta_0 h_{2t}$
Ω_i	$\Omega_0/(1 + \delta_0 h_{2t} K_{i2}/K_{i1})$

TABLE I
PARAMETER SUBSTITUTIONS TO NON-DIMENSIONALIZE THE SYSTEM DEFINED BY (20) INTO (21).

as well as substituting our definition for H_2 from (18) into (20), to arrive at the following system:

$$\begin{aligned}
\frac{d}{d\tau}h_1 &= \frac{\delta_0 h_{1t} h_{2t}/\Omega_0}{1 + \frac{h_1}{\Omega_0} + \frac{x_1}{\Omega_1} + \frac{x_2}{\Omega_2}} - \frac{\delta_0 h_{2t} h_1}{1 + h_1 + x_1 + x_2} \\
\frac{d}{d\tau}x_i &= \delta_i(x_{it} - x_i) - \frac{\alpha_{i1}\delta_0 h_{1t} h_{2t} x_i/\Omega_0}{1 + \frac{h_1}{\Omega_0} + \frac{x_1}{\Omega_1} + \frac{x_2}{\Omega_2}} \\
&\quad - \alpha_{i2} h_{2t} \frac{x_i}{1 + h_1 + x_1 + x_2}.
\end{aligned} \tag{21}$$

Note that Ω_0 is defined exclusively by δ_0 and h_{2t}. The concentration of folded protein i $x_{i,f}$ may be written as:

$$\begin{aligned}
x_{i,f} &= x_{it} - x_i - \frac{x_i h_{1t} \frac{K_0}{K_{i1}} \frac{\delta_0 h_{2t}}{\Omega_0}}{1 + \frac{h_1}{\Omega_0} + \frac{x_1}{\Omega_1} + \frac{x_2}{\Omega_2}} \\
&\quad - \frac{x_i h_{2t} \frac{K_0}{K_{i2}}}{1 + h_1 + x_1 + x_2}.
\end{aligned} \tag{22}$$

For a given state variable x, we denote its equilibrium value by x^*. With fixed x_{it}, $x^*_{i,f}$ is a decreasing function of x^*_i. This system is similar in form to (7); the difference comes in the form of the additional state variable h_1, and the term it brings to the denominator of each refolding term in (21). This leads us to identify a lateral activation effect in our system:

Claim 2. *Let $n = 2$, let θ be a vector containing all parameters in the system and define:*

$$g(\theta) = \left.\frac{\partial x_{1,f}}{\partial x_{2t}}\right|_{x=x^*}.$$

Then, there are θ_0 and θ_1 such that $g(\theta_0) < 0$ and $g(\theta_1) > 0$.

Proof. Let $x = (h_1, x_1, x_2)$, so that $\frac{d}{d\tau}x = f(x) = (\frac{d}{d\tau}h_1, \frac{d}{d\tau}x_1, \frac{d}{d\tau}x_2)$. Then, we consider the system at equilibrium:

$$\begin{aligned}
0 &= \frac{\delta_0 h_{1t} h_{2t}/\Omega_0}{1 + \frac{h_1^*}{\Omega_0} + \frac{x_1^*}{\Omega_1} + \frac{x_2^*}{\Omega_2}} - \frac{\delta_0 h_{2t} h_1^*}{1 + h_1^* + x_1^* + x_2^*} \\
0 &= \delta_i(x_{it} - x_i^*) - \alpha_{i1}\delta_0 h_{1t} h_{2t} \frac{x_i^*/\Omega_0}{1 + \frac{h_1^*}{\Omega_0} + \frac{x_1^*}{\Omega_1} + \frac{x_2^*}{\Omega_2}} \\
&\quad - \alpha_{i2} h_{2t} \frac{x_i^*}{1 + h_1^* + x_1^* + x_2^*}.
\end{aligned}$$

We take the Jacobian of (21) with $x_{2t} = 0$, so that $x_2^* = 0$. With these, the Jacobian evaluates to:

$$\left.\frac{\partial f}{\partial x}\right|_{x=x^*} = \begin{bmatrix} a_{11} & a_{12} & a_{13} \\ a_{21} & a_{22} & a_{23} \\ 0 & 0 & a_{33} \end{bmatrix},$$

where:

$$a_{11} = -\frac{\delta_0 h_{1t} h_{2t}}{\Omega_0^2 c_1^2} - \frac{\delta_0 h_{2t}(1+x_1^*)}{c_2^2} \tag{23}$$

$$a_{ii} = -\delta_{i-1} - \frac{\alpha_{(i-1)1}\delta_0 h_{1t} h_{2t}\left(1+\frac{h_1^*}{\Omega_0}\right)}{\Omega_0 c_1^2} - \frac{\alpha_{(i-1)2} h_{2t}(1+h_1^*)}{c_2^2}, i \in \{2,3\} \tag{24}$$

$$a_{1j} = -\frac{\delta_0 h_{1t} h_{2t}}{\Omega_0 \Omega_{j-1} c_1^2} + \frac{\delta_0 h_1^* h_{2t}}{c_2^2}, j \in \{2,3\} \tag{25}$$

$$a_{2j} = \frac{\alpha_{11}\delta_0 h_{1t} h_{2t} x_1^*}{\Omega_0 \Omega_{j-1} c_1^2} + \frac{\alpha_{12} h_{2t} x_1^*}{c_2^2}, j \in \{1,3\} \tag{26}$$

$$c_1 = 1 + \frac{h_1^*}{\Omega_0} + \frac{x_1^*}{\Omega_1}$$

$$c_2 = 1 + h_1^* + x_1^*.$$

Analysis shows that $\det\left(\frac{\partial f}{\partial x}\right) = a_{11}a_{22}a_{33} - a_{12}a_{21}a_{33} < 0$, so this matrix is invertible. With the implicit function theorem [12], we obtain an expression for $\frac{\partial x}{\partial x_{2t}}$:

$$\left.\frac{\partial x}{\partial x_{2t}}\right|_{x=x^*} = -\left(\frac{\partial f}{\partial x}\right)^{-1}\frac{\partial f}{\partial x_{2t}} \tag{27}$$

$$= -\underbrace{\frac{\delta_2}{\det\left(\frac{\partial f}{\partial x}\right)}}_{>0}\begin{bmatrix} a_{12}a_{23} - a_{13}a_{22} \\ a_{13}a_{21} - a_{23}a_{11} \\ a_{11}a_{22} - a_{12}a_{21} \end{bmatrix}. \tag{28}$$

Taking $\Omega_2 \to 0$, substituting the definitions (23), (25), and (26) into the second row of (28) and simplifying, we arrive at the following expression:

$$\left.\frac{\partial x_1}{\partial x_{2t}}\right|_{x=x^*} = \frac{\delta_0 h_{1t} h_{2t}^2}{\Omega_0 \Omega_2 c_1^2 c_2^2}(\alpha_{11}\delta_0(1+x_1^*) - \alpha_{12}).$$

Since the equilibrium x_1^* is bounded above and below by x_{1t} and 0, respectively, then $\alpha_{12} < \alpha_{11}\delta_0$ implies that the derivative is positive. As was established by (22), $x_{i,f}$ is a decreasing function of x_i under fixed x_{it}, and so we have that $\frac{\partial x_{1,f}}{\partial x_{2t}} < 0$. Similarly, when $\alpha_{12} > \alpha_{11}\delta_0(1+x_{1t})$, then $\frac{\partial x_{1,f}}{\partial x_{2t}} > 0$. Thus we have demonstrated that there are parameter regimes in which $\frac{\partial x_{1,f}}{\partial x_{2t}}$ is positive or negative, completing the proof. □

A parameter sweep to identify regions in which this activating effect is and is not present is shown in Figure 3(a) and validated in Figures 3(b) and 3(c). It is in this fashion that lateral activation manifests: with a sufficiently high affinity for H_1 (Ω_2 small), increasing the total concentration of X_2 leads to the sequestration of both of $\bar{X}_1$'s competitors. Because $\bar{X}_2$ has a high affinity for H_1, it will preferentially bind to this chaperone, shifting the equilibrium away from

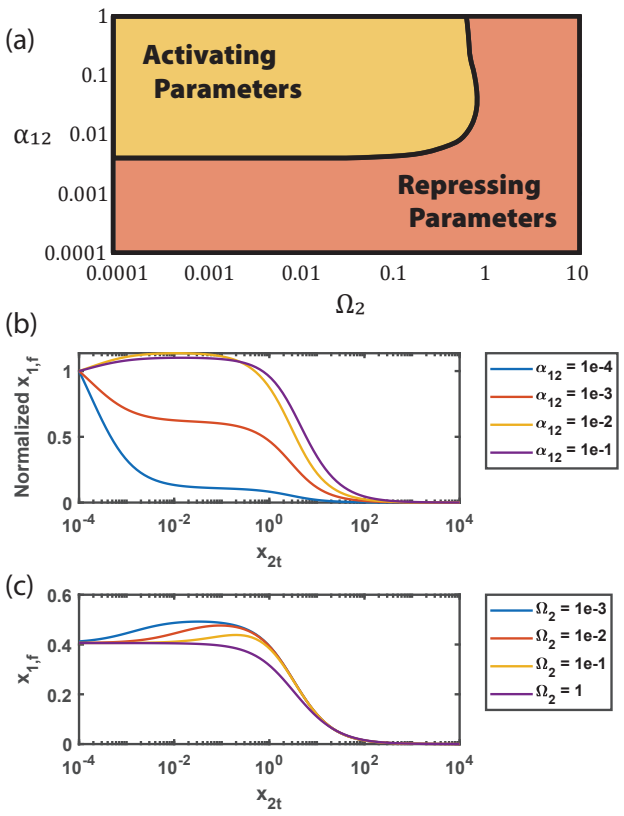

Fig. 3. Modality 2 can exhibit either competitive behavior between different modules, or it can demonstrate a lateral activating behavior. (a) Parameter regimes in which competition or lateral activation are observed. The red-orange region indicates regimes in which the two modules are competitive with each other, so that $\partial x_{1,f}/\partial x_{2t} < 0$, whereas the yellow-orange region indicates regimes in which $\partial x_{1,f}/\partial x_{2t} > 0$. For small Ω_2, the dividing line between the regions is effectively constant in α_{12}, which reflects the boundary conditions on this dividing line provided in Claim 2. Data is obtained from simulations in which $\alpha_{i1} = 0.25$, $\alpha_{22} = 0.05$, $\delta_i = 1$, $h_{1t} = 14$, $h_{2t} = 35$, $\Omega_1 = 72$, and $x_{1t} = 1$. (b,c) Dose response curves confirm that, with sufficiently high α_{12} and sufficiently low Ω_2, a system can display lateral activation, as seen in the fact that $x_{1,f}$ increases in response to an increase in x_{2t}. Eventually, this effect falls apart, as x_{2t} grows large. Data is obtained from simulations using the same parameters as in (a), except that $h_{1t} = 35$, $h_{2t} = 30$, $\Omega_2 = 10^{-4}$ (for (b)), and $\alpha_{12} = 0.05$ (for (c)).

unfolded $\bar{H}_1$, opening up H_2 to fold $\bar{X}_1$. With a sufficiently high folding rate α_{12}, the mutual sequestration of each of $\bar{X}_1$'s competitors leads to a higher folding rate than it would have otherwise achieved. As can be seen in Figures 3(a) and 3(c), however, it is necessary that $\Omega_2 \to 0$, so that this affinity is sufficient to achieve sequestration of the two competitors.

In the previous modality, increasing the concentration of the chaperone would suffice to remove all competition from the system. In this modality, however, this does not occur as before. Individually increasing the concentration of chaperone h_{1t} does appear to reduce the extent of competition between x_1 and x_2, as is visible in Figure 4(a). At the same time, increasing h_{1t} leads to an increase in the occupancy of H_2, reducing the absolute levels of folded protein of interest. Increasing h_{2t} as in Figure 4(b) yields the same analysis as the previous section, in which competition does

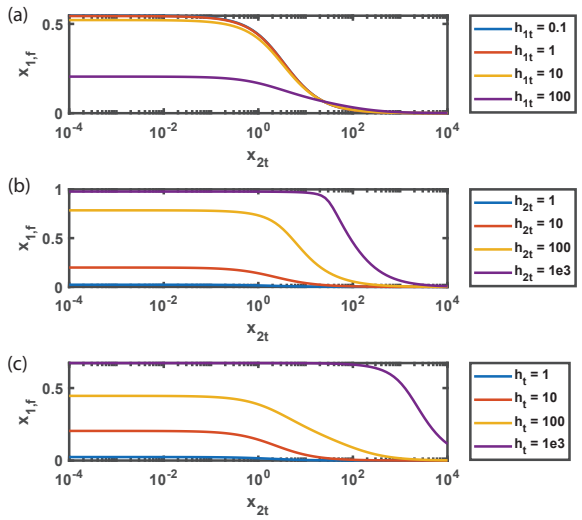

Fig. 4. Competitive effects can be mitigated by increasing h_{2t}, either alone or alongside h_{1t}. (a) Increasing h_{1t} alone does mitigate some of the competitive effects between x_1 and x_2; however, as this chaperone can itself unfold, there is a secondary source of competition as h_{1t} grows large, nullifying the point of introducing more chaperones in the first place. (b,c) Increasing exclusively h_{2t} or both chaperones together mitigates these competition effects. Parameters used are the same as in (a), with $\alpha_{12} = 0.05$, $\Omega_2 = 72$, $h_{2t} = 35$ (for (a)), and $h_{1t} = 14$ (for (b)).

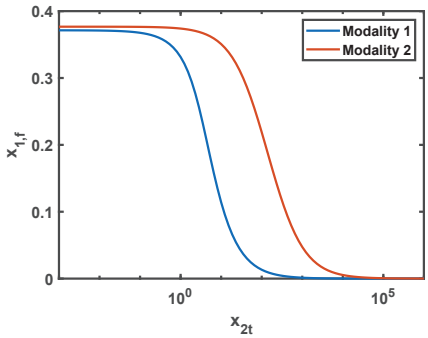

Fig. 5. Comparison of competition extents across the two modalities. The architecture of modality 2 makes it more robust against competition for chaperones compared to modality 1. Parameters used: $\alpha_{i1} = 0.15$, $\delta_2 = 1$, $h_{1t} = 49$, $x_{1t} = 1.32$ for modality 1; $\alpha_{i1} = 0.15$, $\alpha_{i2} = 5 \cdot 10^{-3}$, $\delta_0 = 8.3 \cdot 10^{-3}$, $\delta_i = 1$, $\Omega_i = 72$, $h_{1t} = 14$, $h_{2t} = 35$, $x_{1t} = 100$ for modality 2.

become negligible. Increasing both chaperone concentrations simultaneously keeps the result consistent with the findings from increasing h_{2t} alone (Figure 4(c)).

Figure 5 shows a comparison of the coupling effects of the two modalities for comparable and biologically-reasonable parameter sets, as derived from fitting the model from modality 1 to data from [5]. As can be seen, the lateral activation in modality 2 manifests in a nearly hundredfold increase in x_1's robustness to demands for chaperones by x_{2t} compared to modality 1.

IV. Discussion & Conclusions

There is evidence to suggest that chaperone-reliant proteins compete for folding resources in the cell; however, this relationship has not been characterized extensively [10]. This characterization may be possible by making use of the cell's native heat-shock response system, which is traditionally regulated by a chaperone-binding transcription factor that is deactivated when bound to chaperones [18]. By introducing a fluorescent output at the promoter that this transcription factor regulates, it may be possible to directly observe competition for folding resources.

Chaperones are a critical component of cellular systems, preventing aggregation and ensuring the correct folding of important cellular proteins. As these chaperones are a limited resource in the cell, unintended coupling of genetic circuits because of competition in the cell is a design consideration. In modality 1, this coupling effect was seen to disappear as available chaperone levels increased. In contrast, modality 2 had an architecture that allowed for compensation within a range of competitor levels. In the future, we will consider plausible control architectures that can mitigate the effects of the genetic circuit coupling implicated in this analysis.

References

[1] Hartl, F. Ulrich, Andreas Bracher, and Manajit Hayer-Hartl. "Molecular chaperones in protein folding and proteostasis." Nature 475.7356 (2011): 324-332.

[2] Shemesh, N., Jubran, J., Dror, S. et al. "The landscape of molecular chaperones across human tissues reveals a layered architecture of core and variable chaperones." Nature Communications 12, 2180 (2021).

[3] Wang, Wei, Sandeep Nema, and Dirk Teagarden. "Protein aggregation—Pathways and influencing factors." International journal of Pharmaceutics 390.2 (2010): 89-99.

[4] Santra, Mantu, Daniel W. Farrell, and Ken A. Dill. "Bacterial proteostasis balances energy and chaperone utilization efficiently." Proceedings of the National Academy of Sciences 114.13 (2017): E2654-E2661.

[5] Kerner, Michael J., et al. "Proteome-wide analysis of chaperonin-dependent protein folding in Escherichia coli." Cell 122.2 (2005): 209-220.

[6] Schröder, Hartwig, et al. "DnaK, DnaJ and GrpE form a cellular chaperone machinery capable of repairing heat-induced protein damage." The EMBO Journal 12.11 (1993): 4137-4144.

[7] Qian, Yili, et al. "Resource competition shapes the response of genetic circuits." ACS Synthetic Biology 6.7 (2017): 1263-1272.

[8] Frei, Timothy, et al. "Characterization and mitigation of gene expression burden in mammalian cells." Nature Communications 11.1 (2020): 4641.

[9] Gyorgy, Andras, et al. "Isocost lines describe the cellular economy of genetic circuits." Biophysical Journal 109.3 (2015): 639-646.

[10] Frumkin, Idan and Michael Laub. "Selection of a de novo gene that can promote survival of *Escherichia coli* by modulating protein homeostasis pathways." Nature Ecology and Evolution 7.12 (2023): 2067-2079.

[11] Del Vecchio, Domitilla and Murray, Richard M. *Biomolecular feedback systems.* Princeton University Press, 2014.

[12] J. E. Marsden and M. J. Hoffman, *Elementary Classical Analysis.* 2nd ed., Freeman, 1993.

[13] Ceroni, Francesca, et al. "Burden-driven feedback control of gene expression." Nature methods 15.5 (2018): 387-393.

[14] Fujiwara, Kei, et al. "A systematic survey of in vivo obligate chaperonin-dependent substrates." The EMBO journal 29.9 (2010): 1552-1564.

[15] Deuerling, Elke, et al. "Trigger factor and DnaK cooperate in folding of newly synthesized proteins." Nature 400.6745 (1999): 693-696.

[16] Agashe, Vishwas R., et al. "Function of trigger factor and DnaK in multidomain protein folding: increase in yield at the expense of folding speed." Cell 117.2 (2004): 199-209.

[17] G. Strang, *Linear Algebra and its Applications.* 4th ed., Cengage Learning, 2006.
[18] Narberhaus, Franz, and Sylvia Balsiger. “Structure-function studies of Escherichia coli RpoH (32) by in vitro linker insertion mutagenesis.” Journal of Bacteriology 185.9 (2003): 2731-2738.